ELSEVIER

International Journal of Solids and Structures 41 (2004) 3317–3337

INTERNATIONAL JOURNAL OF SOLIDS and STRUCTURES

www.elsevier.com/locate/ijsolstr

From constitutive modelling of a snow cover to the design of flexible protective structures Part I—Mechanical modelling

François Nicot *

Cemagref, Unité de Recherche Erosion Torrentielle Neige et Avalanches, Domaine Universitaire BP 76, 38402 Saint Martin d Heres, Grenoble, France

Received 5 February 2003; received in revised form 11 September 2003

Available online 26 February 2004

Abstract

The search to improve protective techniques against natural phenomena such as snow avalanches continues to use classic methods to calculate flexible structures. This paper deals with a new method for designing avalanche protection nets, based on a coupled analysis of both the net structure and the snow mantel using a coupled Lagrangian–Discrete approach. As a thorough analysis of the behaviour of a snow cover in interaction with a structure is required, a multiscale approach allowing the overall behaviour of the snowpack to be inferred from the local properties is presented. The constitutive equations are obtained from a statistical description of the mantel, regarded at the micro level as a cohesive granular assembly.

Keywords: Discrete element method; Homogenization; Micro-structure; Multiscale modelling; Snowpack

1. Introduction

1.1. Mountainous areas and snow instabilities

Mountainous areas are generally characterized by strong snow precipitations. Furthermore, these regions have common geomorphological features: erosion has formed a set of valleys whose slopes are often steep. With the effects of gravity, a snow mantel on a slope is likely to develop mechanical instability. Its development depends on several factors such as the rheological properties of the material, the type of soil, the topography, and the climatic conditions. Snow instability induces many natural phenomena characteristic of the mountain environment during winter: avalanches, snow mantel creeping, etc.

* Tel.: +33-4-76-76-27-70; fax: +33-4-76-51-38-03.
E-mail address: francois.nicot@grenoble.cemagref.fr (F. Nicot).

0020-7683/$ - see front matter © 2003 Published by Elsevier Ltd.
doi:10.1016/j.ijsolstr.2003.09.022

1.2. A sensitive socioeconomic context

The Alps remained a relatively isolated region up to the beginning of the 20th century. But industrial and tourist development has led to considerable pressure from local planning needs. Several major roads have also been constructed in Alpine valleys to allow economic exchanges between European countries. Furthermore, because of the presence of water (rivers, streams) associated with the geomorphological features of the area, hydroelectric power plants have been set up along the main rivers. Mining concerns in many areas must also be mentioned. In addition, a substantial industrial network based on electrochemical production has developed to take advantage of these resources.

During this industrial conquest of a part of the Alpine territory, tourist activities increased. In the second part of the last century, urban dwellers began visiting mountain areas for recreational activities: winter tourism, in connection with the surge in skiing, has greatly contributed to this development. In spite of constraints imposed by this particular environment, a large network of infrastructures has been constructed over the past few decades in mountain areas. But these urban facilities are often exposed to hazards such as avalanches. Because avalanches can be highly destructive, the concept of vulnerability must be taken into consideration in these urban areas. Nevertheless, the notion of risk, defined as the product of *vulnerability* per *alea*, has not yet been accepted by society, which has led the fundamental and applied research communities to develop both specific methods and tools to ensure better management of risk.

1.3. A case of active risk intervention: snow avalanche net structures

Risks stemming from snow instabilities can be reduced in different ways. Active risk intervention aims to prevent the failure of the snow mantel and the resulting avalanche; this is possible by stabilizing the snow mantel. Passive intervention does not prevent the triggering of the avalanche, but aims to control the avalanche flowing terms of avalanche direction, velocity, width, and height. Snow avalanche net structures belong to the category of active intervention. This paper deals with modelling the interaction between a snow mantel and this type of structure. Because of their linear shape, snow avalanche net structures are often a well-adapted solution to such problems caused by local topographic conditions. These structures are composed of a set of panels of metallic net, held by poles and anchors (Fig. 1). The downward

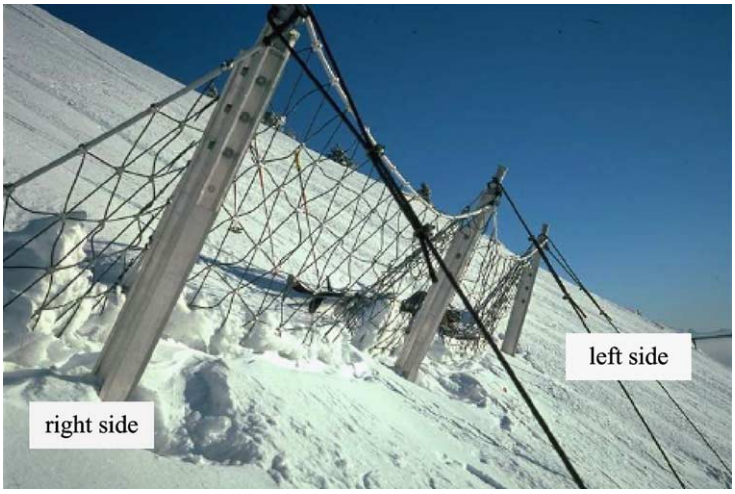

Fig. 1. Example of a snow avalanche net structure (EI Montagne).

movement of the snow mantel is composed of a sliding motion (translation displacement of the entire mantel, considered parallel to the ground surface) and a reptant motion (creeping deformation with settlement). This complex movement directs a strain field and then a stress field into the net sheets. Consequently, a reaction force is applied to the snow mantel; this force results in a stabilization effect.

1.4. Goals and methodology

From a fundamental research point of view, the mechanical interaction between the snow mantel and the structure requires a coupled mechanical analysis. Avalanche net structures are an example of flexible structures. At the equilibrium state, the distribution of forces depends heavily on the strained geometrical shape of the net sheets (Nicot, 1999; Nicot et al., 2002). This feature is the main difference between flexible and rigid structures (Larsen, 2000). The major advantage of our approach is that the final geometrical shape of the net sheets is not assumed; generally, other methods consider a geometrical shape that is not computed, but assessed from in situ observations (Kern, 1978; Margreth, 1995). It is of great interest to predict this final configuration as accurately as possible, because it strongly influences the distribution of forces into the structure. In this context, the new approach introduces the currently used tools and concepts from both solid mechanics (Lemaitre and Chaboche, 1988; Sidoroff, 1984) and numerical modelling (Cundall and Roger, 1992) in order to compute the final geometrical shape. This approach is relevant to the field of avalanche control for the following reasons:

- Initially proposing the final geometrical shape of the structure (net sheets and wires) remains problematic.
- Results from classic methods show that there is a strong relationship between the final geometrical shape and the distribution of internal forces.

Furthermore, the final geometrical shape of the net sheets can be computed only if the loading applied by the snowpack to the structure is correctly described. This requires a thorough description of the behaviour of the snowpack in interaction with the ground, the meteorological conditions, and a flexible or rigid structure.

In what follows, an original method of constitutive modelling of a snowpack will be proposed, based on a multiscale approach allowing the overall behaviour of the snowpack to be inferred from the local properties. Then the case of a snowpack in interaction with an avalanche structure will be considered and a Discrete–Lagrangian approach will be proposed.

2. Constitutive modelling of a snowpack

This paper deals only with snow mantel creeping. As mentioned above, improving defensive structures such as avalanche net structures requires a thorough description of the constitutive behaviour of the snowpack. In the past, many authors have proposed different models using phenomenological approaches (Mellor, 1975; Salm, 1975; Desrues et al., 1980), but these models introduce numerous parameters which are often difficult to calibrate. Similarly, Gagliardini (Gagliardini and Meyssonnier, 1997) has proposed inferring the behaviour of a dense snow mantel from the behaviour of polycrystal ice. The importance of the snow micro-structure to deformational processes has been known for many years (Bader et al., 1939; Kragelski and Shakhov, 1949; Hansen and Brown, 1987; Brown and Edens, 1991). The assessment of the macroscopic properties of a snow mantel from a local description of the micro-structure can be a relevant alternative in as far as the structure at the micro level can be regarded as a granular assembly. Nevertheless, developing a constitutive model using micro-structural properties remains to be done (Lewis et al., 1997).

This paper proposes to develop this kind of multiscale approach, using a statistical description of fabrics. As an application, the case of a snowpack in interaction with a flexible structure is considered.

2.1. Geometric setting

We will consider the case of a snowpack lying on a uniform slope (ψ). It is assumed that the surrounding ground surface can be described by a plane (Π). The set of equations in the following sections will be written in the orthonormal base $(\vec{k}_1, \vec{k}_2, \vec{k}_3)$; (Fig. 2):

$\vec{k}_1$ is the direction of the main slope of (Π);
$\vec{k}_2$ is the horizontal direction of (Π);
$\vec{k}_3$ is the normal direction to the plane (Π).

In this base, coordinates of any point M will be denoted (x_1, x_2, x_3).
We denote L the length of the snowpack, w its width, and H its height. It is assumed that H is uniform.

2.2. General methodology

After snowfalls have occurred, gravity effects occur and the physical structure of the snowpack changes in interaction with the ground and the meteorological conditions. Rather rapidly, initial snow crystals are transformed into ice grains and the resulting snow cover can be considered as a porous material made of ice grains and air (Duva, 1994). Thus, it is assumed in the proposed approach that the snow cover can be described by a sintered granular medium: each ice grain is modelled as a rigid particle. Between neighbouring grains, contacts may occur and solid bonds may be created. Generally, on a small scale, the properties of the materials, whose size is equal to the size of the elementary particles described as rigid bodies, are quite simple (Cambou, 1998). Complexity appears on larger scales (macroscopic scales), because purely geometrical non-linear effects occur inside a large number of particles. As a first approximation, we postulate that the mechanical behaviour of a snow volume element depends only on the mechanical behaviour of inter-granular bonds belonging to this volume. This kind of approach was initially used by Bazant for concrete materials (Bazant and Prat, 1988); more recently, Bartelt has extended this approach to the case of snowpacks (Bartelt and Christen, submitted for publication).

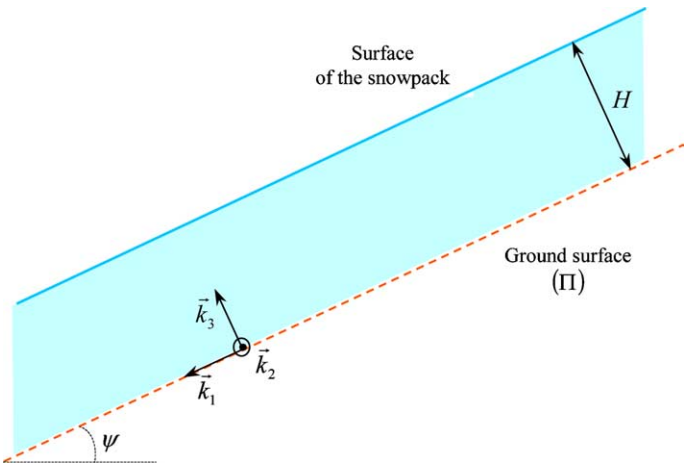

Fig. 2. Definition of the orthonormal base.

The mechanical behaviour of ice bonds can be expressed in a straightforward manner. This paper derives the constitutive behaviour of the snowpack on a macroscopic scale from a microscopic scale description, taking a statistical description of the fabrics into account.

2.3. Microscopic description of the medium

Each ice bond can be described as a tangent thin plane neck. Hereafter, the cross-section of the neck is denoted "contact plane". Under gravity effects, a stress state is generated at each point of the neck. As the magnitude of the neck is very small, the stress state can be assumed to be uniform. This stress state results in a contact force $\vec{F}^c$ whose normal component F_n and the tangential component F_t to the contact plane are expressed as follows:

$$F_n = \tilde{\sigma} S \tag{1}$$

$$F_t = \tilde{\tau} S \tag{2}$$

where $\tilde{\sigma}$ is the normal component and $\tilde{\tau}$ the tangential component of the stress acting in the contact plane, and S is the surface of the cross-section of the neck (Fig. 3).

On the microscopic scale, the behaviour of grain bonds is mainly governed by the behaviour of ice. Several authors such as Meyssonnier and Gagliardini have developed meticulous advanced models for describing the behaviour of ice polycrystals (Gagliardini and Meyssonnier, 1997, 1999). As a first approximation, shear strength is ignored here with regard to compressive or tensile strength. Generally, the local behaviour is described well using a function $\tilde{f}$ relating $\tilde{\sigma}$, $\tilde{\varepsilon}$ and their first time-derivatives $\dot{\tilde{\sigma}}$ and $\dot{\tilde{\varepsilon}}$: $\tilde{f}(\tilde{\sigma}, \dot{\tilde{\sigma}}, \tilde{\varepsilon}, \dot{\tilde{\varepsilon}}) = 0$. For instance, a non-linear visco-elastic tensile–compressive behaviour is described by the well-known relation:

$$\frac{\dot{\tilde{\sigma}}}{K_{ice}} + \left(\frac{\tilde{\sigma}}{\eta_{ice}} \right)^{\alpha_{ice}} = \dot{\tilde{\varepsilon}} \tag{3}$$

where K_{ice} is the Youngs modulus of the ice, and α_{ice} an exponent taking non-linear phenomena into account. When $\alpha_{ice} = 1$, η_{ice} is the viscosity of the ice; otherwise, it is a sort of non-linear viscosity. This non-linear Maxwell model stands as a generalization of Glen's law, which ignores the elastic part of the strain. Glen's law is particularly well adapted to describing creeping phenomena. However, relaxation phenomena are not accounted for by this model. In order to develop a constitutive formulation for snow material that is as general as possible, it would be of interest to consider the non-linear Maxwell model.

In this paper, local strain rates $\dot{\tilde{\varepsilon}}$ are assumed to be large enough (typically, $\dot{\tilde{\varepsilon}} > 10^{-4}\ s^{-1}$) for grain bonds to be regarded as a quasi-brittle material: fracture may occur when grain bonds undergo tensile loading.

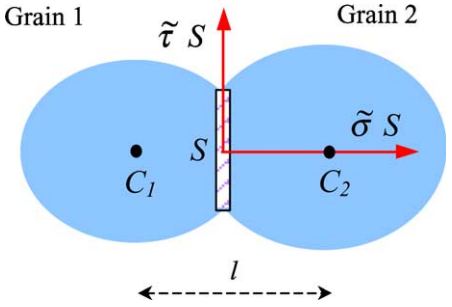

Fig. 3. Ice bond between two grains in contact.

Yield is likely to occur for lower strain rates, but as a first approximation, this case is ignored in this paper. In the case of a snowpack subjected to a creeping deformation, the order of magnitude of local strain rates, which are different from the usual strain rates of a snowpack, is equal to 10^{-3} s^{-1} (Bartelt and Christen, submitted for publication). Thus, the criterion failure can be expressed as follows:

$$\tilde{\sigma} \leqslant \tilde{\sigma}_l \tag{4}$$

where $\tilde{\sigma}_l$ is the failure stress. Ideally, the failure stress should be given as a function of the size of defects taking place within the bonds; assessing the size of defects in terms of reliable local indicators such as stress or geometric parameters is as yet too complex. As a first approach, we consider that the failure stress is uniform within the snowpack because the lack of research in this domain makes a more accurate approach impossible.

Hereafter, for a given snow cover in a given state, it is considered that failure may occur between contact grains. But it is assumed that no new bond can be created between contact grains. Thus, the density of grain bonds is a time-decreasing function.

2.4. Micro–macro description of the medium

2.4.1. Definition of the representative volume element

Hereafter we consider a volume element v_e around a point M, in which the number of grain bonds N_b is large enough so that this volume can be described as a continuous material. Typically, $N_b = 1000$ is a convenient order of magnitude. In such a frame, the normal direction $\vec{n}$ of the different contact planes is assumed to be a continuous variable: point N, defined by $\overrightarrow{ON} = \vec{n}$, describes a half sphere continuously. In the field of granular media, v_e is usually denoted "representative volume element" (RVE) (Masson and Martinez, 2000).

As shown in Fig. 4, the coordinates of $\vec{n}$ can be given as a function of both angles θ (longitude) and φ (colatitude):

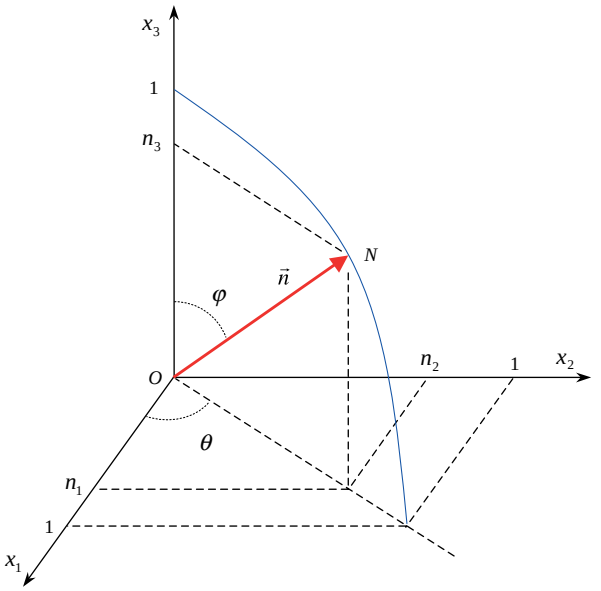

Fig. 4. Continuous description of the normal direction of contact.

$$\vec{n}(\theta,\varphi)=\begin{bmatrix} n_1(\theta,\varphi) \\ n_2(\theta,\varphi) \\ n_3(\theta,\varphi) \end{bmatrix} = \begin{bmatrix} \sin\varphi\cos\theta \\ \sin\varphi\sin\theta \\ \cos\varphi \end{bmatrix} \tag{5}$$

where both θ and φ are continuous variables in $[0,\pi]$.

2.4.2. The macroscopic stress tensor

Considering a representative volume element located around a given point M, the macroscopic stress tensor $\bar{\bar{\sigma}}$ is computed from the local contact forces $\vec{F}^c$ between each pair of ice grains in contact in the RVE. $\bar{\bar{\sigma}}$ and $\vec{F}^c$ can be related by the well-established Love formula of homogenization (Caillerie, 1995):

$$\bar{\bar{\sigma}}_{ij}=\frac{1}{v_e}\sum_c F_i^c l_j^c \tag{6}$$

where F_i^c is the i-component of the contact force $\vec{F}^c$, l_j^c is the j-component of the branch vector $\vec{l}^c$ joining the centres of grains in contact on contact c, and the sum is extended to all the contacts occurring in volume v_e.

As $\vec{F}^c=\tilde{\sigma}(\theta,\varphi)S\vec{n}(\theta,\varphi)$ and $\vec{l}^c=l(\theta,\varphi)\vec{n}(\theta,\varphi)$, Eq. (6) can be rewritten as:

$$\bar{\bar{\sigma}}_{ij}=\frac{1}{v_e}\iint_{[0,\pi]^2} Sl(\theta,\varphi)\tilde{\sigma}(\theta,\varphi)n_i(\theta,\varphi)n_j(\theta,\varphi)\omega(\theta,\varphi)v_e\sin\varphi\,\mathrm{d}\theta\,\mathrm{d}\varphi \tag{7}$$

where $\omega(\theta,\varphi)v_e$ is the number of grain bonds in the direction defined by angles θ and φ and belonging to volume v_e. The length $l(\theta,\varphi)$ between the centres of the two grains in contact is here assumed to be identical for any grain bond, so that $l(\theta,\varphi)=l$ (Fig. 3). Furthermore, $\omega(\theta,\varphi)v_e$ can be related to the probability density $f_{\theta,\varphi}(\theta,\varphi)$ for having a grain bond in direction $\vec{n}_{\bar{\theta},\bar{\varphi}}$ with $\theta<\bar{\theta}<\theta+\mathrm{d}\theta$ and $\varphi<\bar{\varphi}<\varphi+\mathrm{d}\varphi$:

$$f_{\theta,\varphi}(\theta,\varphi)=\frac{\omega(\theta,\varphi)v_e}{N_b} \tag{8}$$

Assuming θ and φ to be statistically independent variables, $f_{\theta,\varphi}$ can be written as the product of both probability densities $f_\theta(\theta)$ and $f_\varphi(\varphi)$:

$$f_{\theta,\varphi}(\theta,\varphi)=f_\theta(\theta)f_\varphi(\varphi) \tag{9}$$

so that Eq. (7) can be rewritten as:

$$\bar{\bar{\sigma}}_{ij}=\iint_{[0,\pi]^2} N_b\frac{Sl}{v_e}\tilde{\sigma}(\theta,\varphi)n_i(\theta,\varphi)n_j(\theta,\varphi)f_\theta(\theta)f_\varphi(\varphi)\sin\varphi\,\mathrm{d}\theta\,\mathrm{d}\varphi \tag{10}$$

Assuming the volume v_g of each ice grain to be approximated by a cylinder, $v_g=lS$, and denoting N_g the number of grains belonging to the RVE, ρ_{ice} the density of ice, and ρ_s the density of the snowpack at the considered point M, the mass balance applied to the RVE provides:

$$N_g v_g \rho_{\mathrm{ice}}=v_e\rho_s \tag{11}$$

Finally, combining both Eqs. (10) and (11) gives:

$$\bar{\bar{\sigma}}_{ij}=\iint_{[0,\pi]^2}\frac{N_b}{N_g}\frac{\rho_s}{\rho_{\mathrm{ice}}}\tilde{\sigma}(\theta,\varphi)n_i(\theta,\varphi)n_j(\theta,\varphi)f_\theta(\theta)f_\varphi(\varphi)\sin\varphi\,\mathrm{d}\theta\,\mathrm{d}\varphi \tag{12}$$

2.4.3. The strain localization relation

Let $\tilde{\sigma}(\theta,\varphi)$ be a statically admissible distribution of stress acting at contact points in the RVE. This distribution directs the distribution of strains $\tilde{\varepsilon}(\theta,\varphi)$, which is then kinematically admissible. The deformation energy $\widetilde{E}(\theta,\varphi)$ associated with the contacts in direction $\vec{n}(\theta,\varphi)$ is given by:

$$\widetilde{E}(\theta,\varphi)=\frac{\omega(\theta,\varphi)v_e}{N_b/v_e}\tilde{\sigma}(\theta,\varphi)\tilde{\varepsilon}(\theta,\varphi) \tag{13}$$

and thus the total deformation energy into an RVE can be written as follows:

$$\widetilde{E}_{\mathrm{d}}=\int\!\!\int_{[0,\pi]^2} v_e\tilde{\sigma}(\theta,\varphi)\tilde{\varepsilon}(\theta,\varphi)f_\theta(\theta)f_\varphi(\varphi)\sin\varphi\,\mathrm{d}\theta\,\mathrm{d}\varphi \tag{14}$$

At the macroscopic level, both distributions $\tilde{\sigma}(\theta,\varphi)$ and $\tilde{\varepsilon}(\theta,\varphi)$ are associated with the macroscopic tensors $\bar{\bar{\sigma}}$ and $\bar{\bar{\varepsilon}}$. The macroscopic deformation energy is given by the following equation:

$$E_{\mathrm{d}}=\sum_{i,j} v_e\bar{\bar{\sigma}}_{ij}\bar{\bar{\varepsilon}}_{ij} \tag{15}$$

Combining Eqs. (12) and (15) provides:

$$E_{\mathrm{d}}=\int\!\!\int_{[0,\pi]^2} v_e\tilde{\sigma}(\theta,\varphi)\sum_{i,j}\left(\frac{N_b}{N_g}\frac{\rho_s}{\rho_{\mathrm{ice}}}\bar{\bar{\varepsilon}}_{ij}n_i(\theta,\varphi)n_j(\theta,\varphi)\right)f_\theta(\theta)f_\varphi(\varphi)\sin\varphi\,\mathrm{d}\theta\,\mathrm{d}\varphi \tag{16}$$

But the "Hill macro homogeneity equality" (Hill, 1967) implies the equality of deformation energies on both scales, thus, $\widetilde{E}_{\mathrm{d}}=E_{\mathrm{d}}$. Given that this relation must be fulfilled only for any statically admissible field and not for any field $\tilde{\sigma}(\theta,\varphi)$ it is not possible to derive the usual result in a rigorous mathematic manner:

$$\tilde{\varepsilon}(\theta,\varphi)=\frac{N_b}{N_g}\frac{\rho_s}{\rho_{\mathrm{ice}}}\sum_{i,j}\bar{\bar{\varepsilon}}_{ij}n_i(\theta,\varphi)n_j(\theta,\varphi) \tag{17}$$

Nevertheless, as an assumption, the expression of local strain given in Eq. (17) will be admitted, but it is an affine approximation of the local strain from the macroscopic strain tensor (Bardet, 1998), which means that the static field $\tilde{\sigma}(\theta,\varphi)$, associated with the strain field $\tilde{\varepsilon}(\theta,\varphi)$ defined with Eq. (17) may not ensure local momentum balance of grain bonds.

In general tensor notations, Eq. (17) can also be rewritten as:

$$\tilde{\varepsilon}(\theta,\varphi)=\frac{N_b}{N_g}\frac{\rho_s}{\rho_{\mathrm{ice}}}(\bar{\bar{\varepsilon}}\circ\vec{n}(\theta,\varphi))\cdot\vec{n}(\theta,\varphi) \tag{18}$$

We denote this relation "the strain localization relation" because it is the local strain in a given direction $\vec{n}(\theta,\varphi)$ defined from the macroscopic strain tensor $\bar{\bar{\varepsilon}}$.

2.4.4. Changes in the medium fabrics

In the proposed approach, the RVE is a statistically homogeneous medium. The location of each ice grain in the RVE is not known, but the direction of grain bonds is statistically described. In this model, the structure at the micro level (fabrics) is completely described by the distribution functions f_θ and f_φ. Initially, just after snowfalls, the spatial distribution of all the grain bonds in the snow cover is approximately isotropic. Rather rapidly, as gravity effects occur, an anisotropy is created, so that the distribution functions are no longer uniform.

We will now investigate a mantel lying on a uniform slope, whose width is much greater than its height, in which the equilibrium metamorphism has occurred; during this metamorphism phase, initial snow crystals are transformed into ice grains and contact bonds may develop between neighbouring grains. We consider that at the end of this development, the state of the mantel can be properly defined by the distribution functions f_θ^0 and f_φ^0, thereby verifying:

$$f_\theta^0(\theta)=\frac{1}{\pi} \tag{19}$$

$$f_{\varphi}^{0}(\pi-\varphi)=f_{\varphi}^{0}(\varphi) \tag{20}$$

The changes in a snowpack will now be analysed from this initial state, which is described by functions f_{θ}^{0} and f_{φ}^{0}. As gravity effects direct a complex downward motion on the snowpack, including creeping and sliding, grain bonds are likely to be broken and the current functions f_{θ} and f_{φ} may change. Thus, in the more general case $f_{\theta}\neq f_{\theta}^{0}$ and $f_{\varphi}\neq f_{\varphi}^{0}$. Eq. (19) means that the directions of contact are equally probable in each plane (x_1,x_2), whereas Eq. (20) means that each plane (x_2,x_3) is a symmetry plane.

The changes in a snowpack in which the rotation of ice grains can be ignored are now the subject of analysis. There is no rotation of the grain bonds if rotation of the grains is ignored; both distribution functions f_{θ} and f_{φ} will evolve depending only on the failure which may occur in grain bonds. From above, the contact in direction $\vec{n}(\theta,\varphi)$ exists while $\tilde{\sigma}(\theta,\varphi)<\tilde{\sigma}_{I}$. From a given state of the medium's fabrics, which is completely described by both distribution functions f_{θ}^{0} and f_{φ}^{0}, it is possible to describe the changes in the medium's fabrics induced by the change in strains. Indeed, current distribution functions f_{θ} and f_{φ} can be easily related to f_{θ}^{0} and f_{φ}^{0}. It is therefore useful to introduce the binary function $\lambda(\theta,\varphi)$, defined as follows:

Initially, $\forall(\theta,\varphi)\ \lambda(\theta,\varphi)=1$

After, as failure may occur, the binary function $\lambda(\theta,\varphi)$ is likely to evolve:

If $\tilde{\sigma}(\theta,\varphi)=\tilde{\sigma}_{I}$ then $\lambda(\theta,\varphi)=0$

Thus,

$$f_{\theta}(\theta)f_{\varphi}(\varphi)=\frac{N_b^0}{N_b}\lambda(\theta,\varphi)f_{\theta}^{0}(\theta)f_{\varphi}^{0}(\varphi) \tag{21}$$

where N_b^0 is the initial number of grain bonds existing in each RVE ($N_b^0\approx 1000$). From Eq. (21), Eq. (12) can be rewritten as:

$$\bar{\bar{\sigma}}_{ij}=\frac{N_b^0}{N_g}\frac{\rho_s}{\rho_{\text{ice}}}\iint_{[0,\pi]^2}\tilde{\sigma}(\theta,\varphi)\lambda(\theta,\varphi)n_i(\theta,\varphi)n_j(\theta,\varphi)f_{\theta}^{0}(\theta)f_{\varphi}^{0}(\varphi)\sin\varphi\,\mathrm{d}\theta\,\mathrm{d}\varphi \tag{22}$$

This expression relates the macroscopic stress tensor to the medium's fabrics.

2.5. Mechanical behaviour of the snowpack on the macro level

2.5.1. General scheme and further approximations

Using previous relations, it is now possible to establish the general scheme, allowing both the macroscopic stress tensor and the strain rate tensor to be related. The scheme depicted in Fig. 4 shows how the stress tensor can be deduced from the strain rate tensor. It must be noted that this scheme is entirely reversible but then requires further appropriate relations to be added. In this paper, the computation of the strain rate tensor from the stress tensor will not be considered.

Whichever local behaviour relates local variables, the scheme proposed in Fig. 5 is consistent and reliable. But non-linear models such as the non-linear visco-elastic tensile–compressive model described by Eq. (3) do not allow an analytical solution to be inferred. In the past, several authors have discussed the

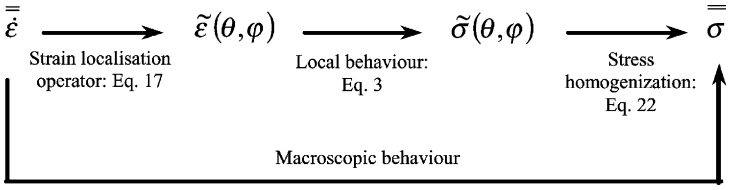

Fig. 5. General scheme relating both the stress tensor and the strain rate tensor.

non-linear properties of ice; even if previous studies have essentially dealt with polar ice, it seems that the behaviour of ice subjected to low stresses could be assumed to be linear, at least as a first approximation (Lliboutry and Duval, 1985; Pimienta, 1987; Castelnau, 1996). The lack of knowledge on the bond-scale structure of the ice makes it difficult to calibrate the exponent α_{ice}. For the purposes of example, analytical constitutive formulation will be proposed considering the linear case: $\alpha_{\text{ice}} = 1$. In the case where $\alpha_{\text{ice}} \neq 1$, only the general form of the constitutive equations will be given. The influence of the exponent α_{ice} will be examined in Part II.

2.5.2. Definition of the constitutive tensor

From the linear Maxwell relation ($\alpha_{\text{ice}} = 1$), $\frac{\dot{\tilde{\sigma}}(\theta,\varphi)}{K_{\text{ice}}} + \frac{\tilde{\sigma}(\theta,\varphi)}{\eta_{\text{ice}}} = \dot{\tilde{\varepsilon}}(\theta,\varphi)$, the expression of $\tilde{\sigma}(\theta,\varphi)$ can be obtained by integration:

$$\tilde{\sigma}(\theta,\varphi) = K_{\text{ice}} \mathrm{e}^{\frac{-K_{\text{ice}}}{\eta_{\text{ice}}}t} \int_0^t \mathrm{e}^{\frac{K_{\text{ice}}}{\eta_{\text{ice}}}\xi} \dot{\tilde{\varepsilon}}(\theta,\varphi)(\xi)\,\mathrm{d}\xi \tag{23}$$

Setting $\phi(\lambda) = \iint_{[0,\pi]^2} \lambda(\theta,\varphi) f_\theta^0(\theta) f_\varphi^0(\varphi) \sin\varphi\,\mathrm{d}\theta\,\mathrm{d}\varphi$, as $N_b = N_b^0 \phi(\lambda)$, combining Eqs. (18), (22), and (23) gives:

$$\begin{aligned}\bar{\bar{\sigma}}_{ij} = \left(\frac{N_b^0}{N_g}\frac{\rho_s}{\rho_{\text{ice}}}\right)^2 \phi(\lambda) K_{\text{ice}} \mathrm{e}^{\frac{-K_{\text{ice}}}{\eta_{\text{ice}}}t} \sum_{k,l} \Bigg\{ \int_0^t \mathrm{e}^{\frac{K_{\text{ice}}}{\eta_{\text{ice}}}\xi} \bar{\bar{\varepsilon}}_{kl}(\xi)\,\mathrm{d}\xi \cdot (\cdots)\ (\cdots) \\ \times \iint_{[0,\pi]^2} \lambda(\theta,\varphi) f_\theta^0(\theta) f_\varphi^0(\varphi) n_i(\theta,\varphi) n_j(\theta,\varphi) n_k(\theta,\varphi) n_l(\theta,\varphi) \sin\varphi\,\mathrm{d}\theta\,\mathrm{d}\varphi \Bigg\}\end{aligned} \tag{24}$$

Let

$$\bar{\bar{\bar{\bar{E}}}}_{kl} = \int_0^t \mathrm{e}^{\frac{K_{\text{ice}}}{\eta_{\text{ice}}}\xi} \dot{\bar{\bar{\varepsilon}}}_{kl}(\xi)\,\mathrm{d}\xi$$

and

$$A_{ijkl} = \iint_{[0,\pi]^2} \lambda(\theta,\varphi) f_\theta^0(\theta) f_\varphi^0(\varphi) n_i(\theta,\varphi) n_j(\theta,\varphi) n_k(\theta,\varphi) n_l(\theta,\varphi) \sin\varphi\,\mathrm{d}\theta\,\mathrm{d}\varphi$$

Thus, on the one hand,

$$\bar{\bar{\sigma}}_{ij} = \left(\frac{N_b^0}{N_g}\frac{\rho_s}{\rho_{\text{ice}}}\right)^2 \phi(\lambda) K_{\text{ice}} \mathrm{e}^{\frac{-K_{\text{ice}}}{\eta_{\text{ice}}}t} \sum_{k,l} A_{ijkl} \bar{\bar{\bar{\bar{E}}}}_{kl} \tag{25}$$

and on the other hand, from both Eqs. (17) and (23):

$$\tilde{\sigma}(\theta,\varphi) = \left(\frac{N_b^0}{N_g}\frac{\rho_s}{\rho_{\text{ice}}}\right) \phi(\lambda) K_{\text{ice}} \mathrm{e}^{\frac{-K_{\text{ice}}}{\eta_{\text{ice}}}t} \sum_{k,l} n_k(\theta,\varphi) n_l(\theta,\varphi) \bar{\bar{\bar{\bar{E}}}}_{kl} \tag{26}$$

A_{ijkl} is a 4-order tensor, denoted "constitutive tensor". Thanks to the symmetry of both $\bar{\bar{\sigma}}_{ij}$ and $\bar{\bar{\varepsilon}}_{ij}$ tensors, A_{ijkl} can be contracted into a symmetric 6×6 matrix M_{ij} relating these vectors $\bar{\sigma}_i = [\sigma_{11}, \sigma_{22}, \sigma_{33}, \sqrt{2}\sigma_{12}, \sqrt{2}\sigma_{13}, \sqrt{2}\sigma_{23}]$ and $\bar{E}_i = [E_{11}, E_{22}, E_{33}, \sqrt{2}E_{12}, \sqrt{2}E_{13}, \sqrt{2}E_{23}]$:

$$M_{ij} = \begin{bmatrix} A_{1111} & A_{2211} & A_{3311} & \sqrt{2}A_{1211} & \sqrt{2}A_{1311} & \sqrt{2}A_{2311} \\ A_{1122} & A_{2222} & A_{3322} & \sqrt{2}A_{1222} & \sqrt{2}A_{1322} & \sqrt{2}A_{2322} \\ A_{1133} & A_{2233} & A_{3333} & \sqrt{2}A_{1233} & \sqrt{2}A_{1333} & \sqrt{2}A_{2333} \\ \sqrt{2}A_{1112} & \sqrt{2}A_{2212} & \sqrt{2}A_{3312} & 2A_{1212} & 2A_{1312} & 2A_{2312} \\ \sqrt{2}A_{1113} & \sqrt{2}A_{2213} & \sqrt{2}A_{3313} & 2A_{1213} & 2A_{1313} & 2A_{2313} \\ \sqrt{2}A_{1123} & \sqrt{2}A_{2223} & \sqrt{2}A_{3323} & 2A_{1223} & 2A_{1323} & 2A_{2323} \end{bmatrix} \tag{27}$$

The following constitutive relationship is finally obtained:

$$\bar{\sigma}_i = \left(\frac{N_b^0}{N_g}\frac{\rho_s}{\rho_{\text{ice}}}\right)^2 \phi(\lambda) K_{\text{ice}} \mathrm{e}^{\frac{-K_{\text{ice}}}{\eta_{\text{ice}}}t} \sum_j M_{ij}\overline{E}_j \tag{28}$$

$\overline{\overline{M}}_{ij}$ is denoted the "constitutive matrix" and the term $C_{\text{h}} = \left(\frac{N_b^0}{N_g}\frac{\rho_s}{\rho_{\text{ice}}}\right)^2 \phi(\lambda)$ is a homogenization coefficient, which is generally lower than 1.

2.5.3. Calculation of the constitutive matrix

In order to exemplify the form of the matrix $\overline{\overline{M}}_{ij}$, the different terms are calculated considering the initial state of the snowpack ($f_\theta = f_\theta^0$ and $f_\varphi = f_\varphi^0$). In this case, for any values of θ and φ, $\lambda(\theta, \varphi)$ is equal to 1. It may be established that the constitutive matrix can be written as follows:

$$\overline{\overline{M}} = \begin{bmatrix} \frac{3}{8}S_5 & \frac{1}{8}S_5 & \frac{1}{2}(S_3 - S_5) & 0 & 0 & 0 \\ \frac{1}{8}S_5 & \frac{3}{8}S_5 & \frac{1}{2}(S_3 - S_5) & 0 & 0 & 0 \\ \frac{1}{2}(S_3 - S_5) & \frac{1}{2}(S_3 - S_5) & 1 - 2S_3 + S_5 & 0 & 0 & 0 \\ 0 & 0 & 0 & \frac{1}{4}S_5 & 0 & 0 \\ 0 & 0 & 0 & 0 & S_3 - S_5 & 0 \\ 0 & 0 & 0 & 0 & 0 & S_3 - S_5 \end{bmatrix} \tag{29}$$

where S_p stands for a p-order moment of distribution function f_φ^0:

$$S_p = \int_0^\pi f_\varphi^0(\varphi) \sin^p \varphi \, \mathrm{d}\varphi \tag{30}$$

It must be noted that $\overline{\overline{M}}_{ij}$ is a pseudo-isotropic transverse matrix, with only two independent coefficients.

Furthermore, if the distribution function f_φ^0 is assumed to be uniform, as $\int_0^\pi f_\varphi^0(\varphi) \sin\varphi \, \mathrm{d}\varphi = 1$, it follows that $f_\varphi^0(\varphi) = 1/2$; the different values of S_p can be directly calculated: $S_3 = 2/3$ and $S_5 = 8/15$.

Thus, as depicted in Eq. (31), $\overline{\overline{M}}_{ij}$ is a perfectly isotropic matrix. This result is absolutely consistent, because the material structure of the snowpack is also isotropic.

$$\overline{\overline{M}} = \frac{1}{15}\begin{bmatrix} 3 & 1 & 1 & 0 & 0 & 0 \\ 1 & 3 & 1 & 0 & 0 & 0 \\ 1 & 1 & 3 & 0 & 0 & 0 \\ 0 & 0 & 0 & 2 & 0 & 0 \\ 0 & 0 & 0 & 0 & 2 & 0 \\ 0 & 0 & 0 & 0 & 0 & 2 \end{bmatrix} \tag{31}$$

2.5.4. Asymptotic behaviour

Interestingly, in order to examine the structure of the constitutive model, a simplistic case is considered. In the general case, this constitutive model was recently more thoroughly analysed by Nicot (submitted for publication). If the viscosity of ice is supposed to be infinite, the behaviour of the material becomes a purely

quasi-brittle elastic behaviour. Eq. (28) can be rewritten as $\bar{\sigma}_i = C_h K_{ice} \sum_j M_{ij} \bar{\varepsilon}_j$ with $\bar{\varepsilon}_i = [\varepsilon_{11}, \varepsilon_{22}, \varepsilon_{33}, \sqrt{2}\varepsilon_{12}, \sqrt{2}\varepsilon_{13}, \sqrt{2}\varepsilon_{23}]$. It must be noted that each term of the matrix of elasticity is the product of the Youngs modulus of ice K_{ice} by the homogenization coefficient and the term $\overline{\overline{M}}_{ij}$, which depends only on the distribution functions f_θ and f_φ. In the particular case where the medium may be isotropic ($f_\theta(\theta) = 1/\pi$ and $f_\varphi(\varphi) = 1/2$), the behaviour is also isotropic. This requires the failure stress $\tilde{\sigma}_l$ to be infinite. In this case, the equation $\bar{\sigma}_i = C_h K_{ice} \sum_j M_{ij} \bar{\varepsilon}_j$ can also be expressed in the following manner, $\sigma_{ij} = \frac{C_h K_{ice}}{15}(2\varepsilon_{ij} + tr(\bar{\bar{\varepsilon}})\delta_{ij})$, allowing Lame's constants μ and λ to be calculated: $\lambda = \mu = C_h K_{ice}/15$. Thus, the global Young modulus K_s and Poisson coefficient v_s can be inferred for the medium on the macro level: $K_s = \frac{C_h}{6} K_{ice}$ and $v_s = 1/4$. It must be noted that these results are in perfect agreement with those obtained by other authors (Chang and Liao, 1994; Cambou et al., 1995), when the local tangential stiffness is ignored.

3. Application to the case of a snowpack in interaction with an avalanche structure

3.1. The constitutive relation for the snowpack

3.1.1. The macroscopic strain

The snowpack is composed of n_l layers, whose height (h_l) and length (L) are uniform. Each layer is associated with a meteorological event: both density ρ_l and mechanical parameters related to the mantel are assumed to be uniform within each layer 'l'. The height of the entire mantel is given by the relation:

$$H = \sum_{l=1}^{n_l} h_l \tag{32}$$

Width w is assumed to be substantially greater than both height H and length L. Thus, by denoting (u_1, u_2, u_3) the components of the displacement field $\vec{u}$, u_2 can be ignored with regard to both u_1 and u_3. Furthermore, as a first approximation, component u_1 does not depend on position x_1. Also assuming that the structure does not substantially modify the settlement of the snowpack, it can be postulated that u_3 does not depend on positions x_1 and x_2. Finally, the displacement field can be defined as follows:

$$\vec{u} = \begin{bmatrix} u_1(x_2, x_3, t) \\ 0 \\ u_3(x_3, t) \end{bmatrix} \tag{33}$$

In these conditions, the strain rate tensor $\dot{\bar{\bar{\varepsilon}}}$, for small deformation, is given by:

$$\dot{\bar{\bar{\varepsilon}}} = \begin{bmatrix} 0 & \frac{1}{2}\frac{\partial \dot{u}_1}{\partial x_2} & \frac{1}{2}\frac{\partial \dot{u}_1}{\partial x_3} \\ \frac{1}{2}\frac{\partial \dot{u}_1}{\partial x_2} & 0 & 0 \\ \frac{1}{2}\frac{\partial \dot{u}_1}{\partial x_3} & 0 & \frac{\partial \dot{u}_3}{\partial x_3} \end{bmatrix} \tag{34}$$

From a physical point of view, both height and density profiles are time dependent; but in the proposed approach, the settlement phenomenon is assumed not to have a strong interaction with the creeping phenomenon. Furthermore, it seems to be relevant to consider that the loading applied by the snowpack to the structure is mainly caused by the creeping phenomenon, and not by the settlement phenomenon. Thus, the creeping phenomenon is investigated by taking into account the final values of height H and density ρ_l. These data can be assessed by specific numerical tools such as CROCUS (Brun et al., 1989). This implies that any point M belonging to the snowpack is subjected to a displacement $\vec{u} = u_1(x_2, x_3, t)\vec{k}_1$ in a single

direction ($\vec{k}_1$), which only depends on coordinates x_2 and x_3. Thus, the considered strain rate tensor has the following form:

$$\dot{\bar{\bar{\varepsilon}}} = \begin{bmatrix} 0 & \frac{1}{2}\frac{\partial \dot{u}_1}{\partial x_2} & \frac{1}{2}\frac{\partial \dot{u}_1}{\partial x_3} \\ \frac{1}{2}\frac{\partial \dot{u}_1}{\partial x_2} & 0 & 0 \\ \frac{1}{2}\frac{\partial \dot{u}_1}{\partial x_3} & 0 & 0 \end{bmatrix} \tag{35}$$

Furthermore, a numerical tool such as CROCUS enables both the initial mean coordination number $\bar{n}_c$ and the mean volume v_g of ice grains to be assessed; this allows both N_g and N_b^0 to be related as: $N_b^0 = \bar{n}_c N_g$, and thus, taking Eq. (11) into account, the RVE can be deduced with the following equation:

$$v_e = v_g \frac{N_b^0}{\bar{n}_c} \frac{\rho_{\text{ice}}}{\rho_l} \tag{36}$$

It must be noted that ρ_l, as well as $\bar{n}_c$, may be a function of the considered position (point M).

3.1.2. The constitutive formulation

3.1.2.1. The linear case. In the most general case, function $\lambda(\theta, \varphi)$ is equal to 0 or 1, so that the general expression of $\overline{\overline{M}}$ given by Eq. (27) has to be considered. In order to exemplify the constitutive formulation, the distribution function f_φ is assumed to be uniform, so that $f_\varphi^0(\varphi) = 1/2$ for any value of φ. From Eq. (28), making use of the particular form of the strain rate tensor given in Eq. (35), the following relation can be derived:

$$\bar{\sigma}_i = 2C_{\text{h}} K_{\text{ice}} \mathrm{e}^{\frac{-K_{\text{ice}}}{\eta_{\text{ice}}} t} \left(\overline{\overline{M}}_{i4} \int_0^t \mathrm{e}^{\frac{K_{\text{ice}}}{\eta_{\text{ice}}} \xi} \dot{\bar{\bar{\varepsilon}}}_{12} \, \mathrm{d}\xi + \overline{\overline{M}}_{i5} \int_0^t \mathrm{e}^{\frac{K_{\text{ice}}}{\eta_{\text{ice}}} \xi} \dot{\bar{\bar{\varepsilon}}}_{13} \, \mathrm{d}\xi \right) \quad (i = 1, \ldots, 6) \tag{37}$$

In particular, the two shear terms are given by:

$$\bar{\bar{\sigma}}_{12} = 2C_{\text{h}} K_{\text{ice}} \mathrm{e}^{\frac{-K_{\text{ice}}}{\eta_{\text{ice}}} t} \left(\overline{\overline{M}}_{44} \int_0^t \mathrm{e}^{\frac{K_{\text{ice}}}{\eta_{\text{ice}}} \xi} \dot{\bar{\bar{\varepsilon}}}_{12} \, \mathrm{d}\xi + \overline{\overline{M}}_{45} \int_0^t \mathrm{e}^{\frac{K_{\text{ice}}}{\eta_{\text{ice}}} \xi} \dot{\bar{\bar{\varepsilon}}}_{13} \, \mathrm{d}\xi \right) \tag{38}$$

and

$$\bar{\bar{\sigma}}_{13} = 2C_{\text{h}} K_{\text{ice}} \mathrm{e}^{\frac{-K_{\text{ice}}}{\eta_{\text{ice}}} t} \left(\overline{\overline{M}}_{54} \int_0^t \mathrm{e}^{\frac{K_{\text{ice}}}{\eta_{\text{ice}}} \xi} \dot{\bar{\bar{\varepsilon}}}_{12} \, \mathrm{d}\xi + \overline{\overline{M}}_{55} \int_0^t \mathrm{e}^{\frac{K_{\text{ice}}}{\eta_{\text{ice}}} \xi} \dot{\bar{\bar{\varepsilon}}}_{13} \, \mathrm{d}\xi \right) \tag{39}$$

The calculation of terms $\overline{\overline{M}}_{44}$, $\overline{\overline{M}}_{45}$ and $\overline{\overline{M}}_{55}$ requires knowing the function $\lambda(\theta, \varphi)$. This function is related to the microscopic stress $\tilde{\sigma}(\theta, \varphi)$, whose expression is given by Eq. (26). As only the two terms $\bar{\bar{E}}_{12}$ and $\bar{\bar{E}}_{13}$ are not nil, it can be inferred that:

$$\tilde{\sigma}(\theta, \varphi) = \sqrt{2} \left(\frac{N_b^0}{N_g} \frac{\rho_s}{\rho_{\text{ice}}} \right) \phi(\lambda) K_{\text{ice}} \mathrm{e}^{\frac{-K_{\text{ice}}}{\eta_{\text{ice}}} t} \left(n_1(\theta, \varphi) n_2(\theta, \varphi) \bar{\bar{E}}_{12} + n_1(\theta, \varphi) n_3(\theta, \varphi) \bar{\bar{E}}_{13} \right) \tag{40}$$

and taking into account Eq. (5), this expression can be rewritten as:

$$\tilde{\sigma}(\theta, \varphi) = C_{12} \cos\theta \sin\theta \sin^2\varphi + C_{13} \cos\theta \cos\varphi \sin\varphi \tag{41}$$

where

$$C_{1i} = 2 \left(\frac{N_b^0}{N_g} \frac{\rho_s}{\rho_{\text{ice}}} \right) \phi(\lambda) K_{\text{ice}} \mathrm{e}^{\frac{-K_{\text{ice}}}{\eta_{\text{ice}}} t} \int_0^t \mathrm{e}^{\frac{K_{\text{ice}}}{\eta_{\text{ice}}} \xi} \dot{\bar{\bar{\varepsilon}}}_{1i} \, \mathrm{d}\xi \quad (i = 1, 2) \tag{42}$$

3.1.2.2. The non-linear case. Given both terms $\dot{\bar{\bar{\varepsilon}}}_{12}$ and $\dot{\bar{\bar{\varepsilon}}}_{13}$, from Eq. (10), the local strain rate is given by:

$$\dot{\tilde{\varepsilon}}(\theta,\varphi) = \left(\frac{N_b^0}{N_g}\frac{\rho_s}{\rho_{\text{ice}}}\right)\phi(\lambda)\left(\dot{\bar{\bar{\varepsilon}}}_{12}\sin^2\varphi\cos\theta\sin\theta + \dot{\bar{\bar{\varepsilon}}}_{13}\cos\varphi\sin\varphi\cos\theta\right) \tag{43}$$

Thus, the local stress is obtained with numerical integration of differential equation

$$\frac{\dot{\tilde{\sigma}}(\theta,\varphi)}{K_{\text{ice}}} + \left(\frac{\tilde{\sigma}(\theta,\varphi)}{\eta_{\text{ice}}}\right)^{\alpha_{\text{ice}}} = \dot{\tilde{\varepsilon}}(\theta,\varphi)$$

This makes it possible to infer a numerical estimate of $\lambda(\theta,\varphi)$, and thus of $\bar{\bar{\sigma}}_{12}$ and $\bar{\bar{\sigma}}_{13}$:

$$\bar{\bar{\sigma}}_{12} = \frac{1}{2\pi}\left(\frac{N_b^0}{N_g}\frac{\rho_s}{\rho_{\text{ice}}}\right)\iint_{[0,\pi]^2}\tilde{\sigma}(\theta,\varphi)\lambda(\theta,\varphi)\cos\theta\sin\theta\sin^3\varphi\,\mathrm{d}\theta\,\mathrm{d}\varphi \tag{44}$$

and

$$\bar{\bar{\sigma}}_{13} = \frac{1}{2\pi}\left(\frac{N_b^0}{N_g}\frac{\rho_s}{\rho_{\text{ice}}}\right)\iint_{[0,\pi]^2}\tilde{\sigma}(\theta,\varphi)\lambda(\theta,\varphi)\cos\theta\cos\varphi\sin^2\varphi\,\mathrm{d}\theta\,\mathrm{d}\varphi \tag{45}$$

As a general analytical solution of Eq. (3) does not exist, an analytical solution relating $\dot{\bar{\bar{\varepsilon}}}_{12}$ and $\dot{\bar{\bar{\varepsilon}}}_{13}$ with $\bar{\bar{\sigma}}_{12}$ and $\bar{\bar{\sigma}}_{13}$ cannot be derived. Contrary to the linear case, this means that the analytical expression of the constitutive matrix $\overline{\overline{M}}$ cannot be inferred.

3.2. Spatial description of the bodies

3.2.1. Phenomenological analysis

The downward movement of the snow mantel is composed of a gliding motion (translation displacement of the entire mantel considered, parallel to the ground surface) and of a reptant motion (creeping deformation with settlement). In the course of the creeping deformation, complex changes in the micro-structure take place, which strongly govern the distribution of internal stresses (Kry, 1975). As indirect evidence, recorded acoustic emissions show that grain bonds may fail (St. Lawrence, 1980). Thus, the multiscale constitutive model presented in the previous sections seems to be well adapted to the analysis of the downward movement of a snowpack.

The purpose of open structures such as snow avalanche nets is not to prevent the downward motion of the snowpack. The practical objective is to slow down this motion in order to reduce the stresses existing in the snowpack. This strongly limits the risk of initialization of large-scale failure mechanisms. The slowdown results mainly from the friction between the snow cover and both the wires of the net sheet and the poles. Other phenomena may occur at the interface between the wires and the snow, induced in part by the thermal conductivity of metallic wires; but these are second-order phenomena that can be ignored as a first assumption.

3.2.2. The snowpack

Any point M belonging to the snowpack is subjected to a displacement in a single direction ($\vec{k}_1$). Thus, each layer of the snow mantel can be described by a regular set of rigid parallelepiped elements (snow elements), which remain parallel to direction $\vec{k}_1$. By denoting h_e, w_e, and L, respectively, as the height, the width and the length of each snow element 'e', the volume V_e is given by the relation:

$$V_e = h_e w_e L \tag{46}$$

It must be noted that the typical size of h_e (resp. w_e) is very small with regard to the size of H (resp. w). But the RVE must also be entirely contained in a snow element; this requirement must be fulfilled in order to use the previous constitutive model, making the following condition necessary:

$$\min(h_e, w_e) > \left(\frac{3}{4\pi} v_e\right)^{1/3} \tag{47}$$

Eq. (36) expresses v_e as a function of the following parameters, whose usual values or ranges can be given: $N_b^0 = 1000$, $2 \leqslant \bar{n}_c \leqslant 5$, $\rho_{\text{ice}} = 915$ kg/m^3, $150 \leqslant \rho_l \leqslant 550$ (kg/m^3), with the diameter of the ice grains equal to 0.002 m. Table 1 gives the mean value of the equivalent radius of the RVE (corresponding to $\rho_l = 350$ kg/m^3 and $\bar{n}_c = 3.5$), its minimal value (corresponding to $\rho_l = 550$ kg/m^3 and $\bar{n}_c = 5$), and its maximal value (corresponding to $\rho_l = 150$ kg/m^3 and $\bar{n}_c = 2$). Consequently, if the value of $\min(h_e, w_e)$ is chosen greater than 0.02 m, the condition indicated in Eq. (47) is automatically fulfilled.

The snow elements are in contact with each other and may slide downstream (Fig. 6). The constitutive behaviour of the snowpack is modelled by a shear contact law, allowing the contact between each pair of adjoining snow elements to be described.

3.2.3. The snow avalanche structure

3.2.3.1. Technological elements of the structure. The snow avalanche structure is composed of several panels of net sheet, connected to both the upstream anchors and the poles. The net sheet is composed of a set of metallic net panels (Fig. 7). Initially, each panel has an isosceles geometrical shape, defined by three perimeter wires. The base side is distinguished from the two lateral sides. The three vertices of every panel are connected to both the poles and the upstream anchors. The poles are stabilized with the downstream wires, which are connected to downstream anchors. Each metallic net panel is composed of a regular mesh of intersected metallic wires. These wires are fixed at each connection point. It will be assumed that each single wire belonging to the strained sheet keeps a linear geometrical shape between two intersection points.

3.2.3.2. Spatial description. The net sheet can be described by a set of nodes located at the intersection points between single wires (Fig. 8). The straight lines which appear in Fig. 8 between each pair of adjoining nodes are merely fictitious: the structure is completely described by a set of nodes. This means that the

Table 1
Variations in the equivalent radius

	Minimal value	Mean value	Maximal value
Equivalent radius $\left(\frac{3}{4\pi} v_e\right)^{1/3}$	0.69 cm	0.91 cm	1.45 cm

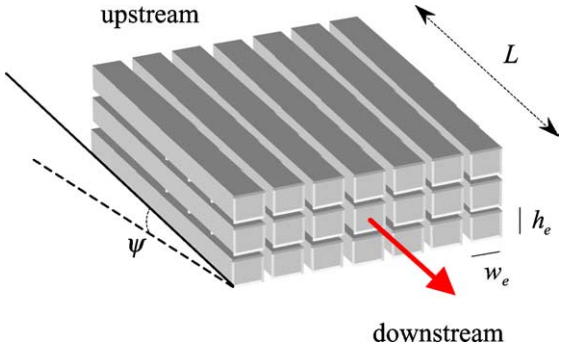

Fig. 6. Spatial description of the snow mantel.

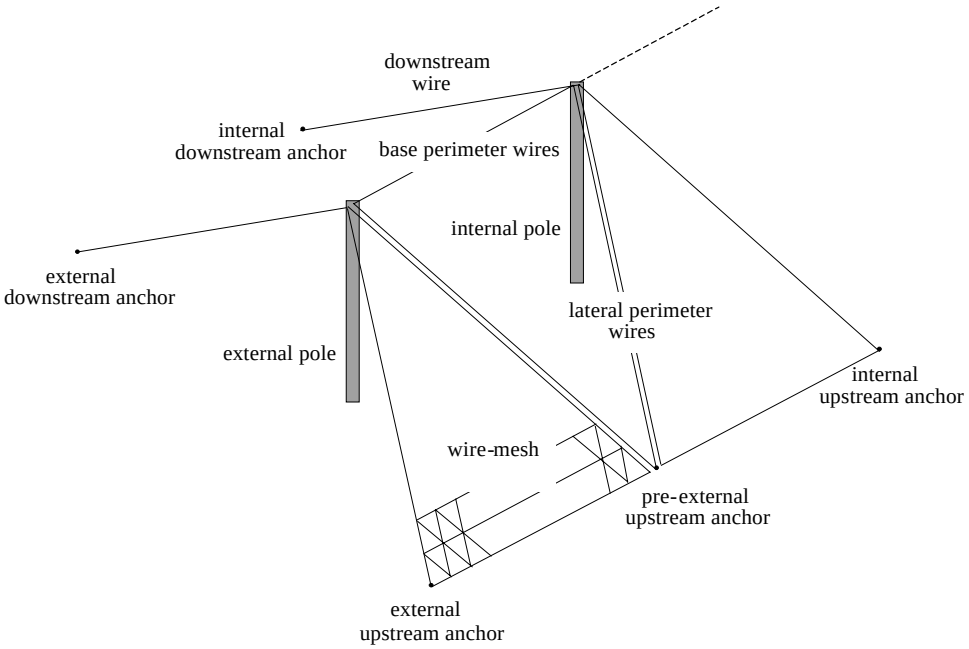

Fig. 7. Wordlist of snow avalanche net structures.

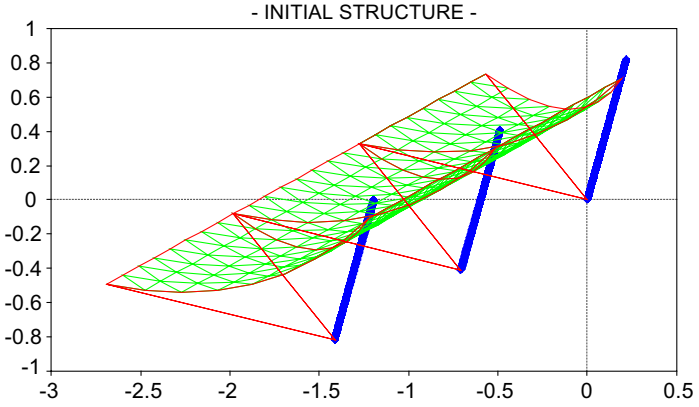

Fig. 8. Spatial description of avalanche net structure.

contact between the snowpack and the net sheet will occur only at the nodes of the mesh and not along the lines joining the nodes. The nodes located at the connection points between the net sheet and the poles or the anchors will be assumed to be fixed. Even if the structure gives rise to considerable deformation, it must be noted that strains within every individual wire remain very limited. Thus, the behaviour of wires belongs to the elastic domain. In this approach, the mass of the net sheet is equally concentrated on each node, whose mass is denoted m. Initially, as suggested in Fig. 8, the net sheet is assumed to have a paraboloidal shape.

3.3. Mechanical description

3.3.1. Lagrangian description of the snowpack

Each snow element I, which belongs to the layer l, is in contact with four other neighbouring elements I_n (Fig. 9). It is subjected to the action of both its weight and a set of four contact forces T_I^n. If this element is in contact with a node belonging to the net sheet, it is also subjected to the reaction force R_I.

The main feature of this approach, which is explicit in time, is to follow the behaviour of each snow element during its movement. Contrary to a discrete description, the contact forces between each pair of neighbouring elements are calculated from a continuous formulation relating the shear stress to the shear strain rate. Thus, using the definition given by Billaux and Cundall (Billaux, 1993), this approach is considered to be Lagrangian.

The kinematics of each snow element is completely described by a single parameter u_I (henceforth the subscript 1 will be omitted from term u), which represents the total displacement of element I in direction $\vec{k}_1$. The displacement u_I of snow element I belonging to the layer l, is given by Eq. (48). If this element is not in contact with a node belonging to the net sheet, the reaction force R_I is nil: $R_I = 0$. In this case, the snow element flows through the net sheet.

$$\rho_l V_e \ddot{u}_I = \rho_l V_e g \sin\psi + \sum_{n=1}^{4} T_I^n - R_I \tag{48}$$

If the snow element is located upstream from a pole, Eq. (48) remains valid by setting $u_I = 0$; the snow element is blocked, and a reaction force $R_I = \rho_l V_e g \sin\psi + \sum_{n=1}^{4} T_I^n$ appears between this element and the pole. Reaction forces existing between a pole and the snow elements in contact allow the pressure applied by the snow mantel to the pole to be assessed.

The contact force T_I^n is computed by integrating the shear stress along the surface at the interface of the two neighbouring elements I and I_n. To exemplify this, let us now consider the case of the two elements I and I_1. The shear stress $\bar{\bar{\sigma}}_{13}(I, I_1)$ existing at the interface of the two elements can be assessed by interpolation between points A and B (Fig. 10):

$$\bar{\bar{\sigma}}_{13}(I, I_1) = \tfrac{1}{2}(\bar{\bar{\sigma}}_{13}(A) + \bar{\bar{\sigma}}_{13}(B)) \tag{49}$$

and thus the contact force T_I^1 between the two elements I and I_1 can be easily deduced:

$$T_I^1 = L w_e \bar{\bar{\sigma}}_{13}(I, I_1) \tag{50}$$

From general equations (43)–(45), $\bar{\bar{\sigma}}_{13}$ depends only on $\bar{\bar{\varepsilon}}_{12}$ and $\bar{\bar{\varepsilon}}_{13}$. These two terms can be assessed from the displacements of the elements belonging to the common neighbourhood of I and I_1 (Fig. 10).

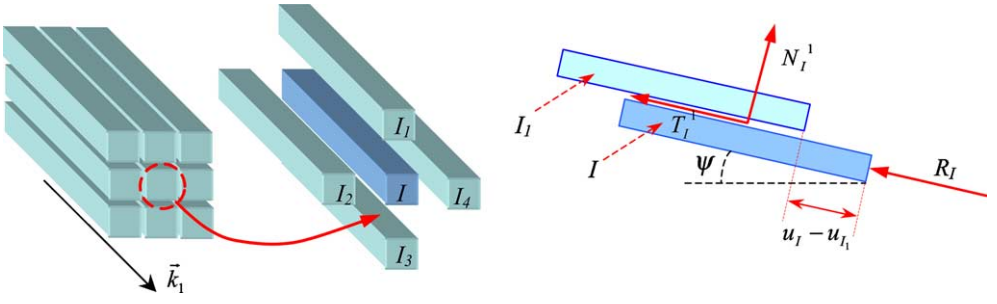

Fig. 9. Description of snow elements.

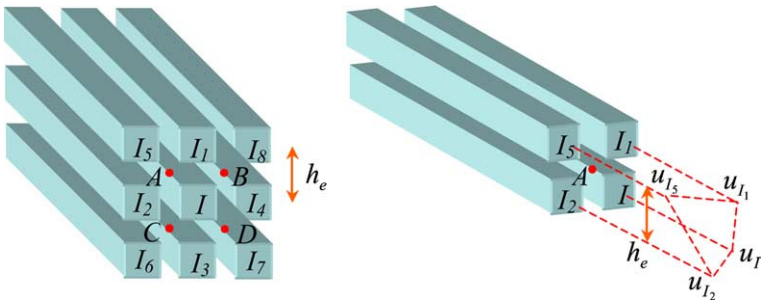

Fig. 10. Lagrangian description of snow elements.

Indeed, the shear strain $\bar{\bar{\varepsilon}}_{13}(A)$ at point A, for instance, located at the centre of the four elements I, I_1, I_2, and I_5, can be assessed by the following formulation using the Gauss approximation (Billaux, 1993):

$$\bar{\bar{\varepsilon}}_{13}(A) \approx \frac{1}{2}\left(\frac{u_{I_1}-u_I}{h_e}+\frac{u_{I_5}-u_{I_2}}{h_e}\right) \tag{51}$$

Likewise, the shear strain $\bar{\bar{\varepsilon}}_{13}(B)$ at point B is given by:

$$\bar{\bar{\varepsilon}}_{13}(B) \approx \frac{1}{2}\left(\frac{u_{I_1}-u_I}{h_e}+\frac{u_{I_8}-u_{I_4}}{h_e}\right) \tag{52}$$

The same method can be used to compute the three other terms T_I^2, T_I^3 and T_I^4.

3.3.2. Discrete description of the net structure

Each node J belonging to the net sheet is connected to six neighbouring nodes J_p (Fig. 11). In every fictitious individual wire, joining neighbouring nodes J and J_p acts an elastic force F_J^p.

The vectorial location $\vec{X}_J$ of node J (mass m), in contact with snow element I, is given by Eq. (53):

$$m\ddot{\vec{X}}_J = m\vec{g} + \sum_{p=1}^{6}\vec{F}_J^p + R_I\vec{k}_1 \tag{53}$$

with

$$\vec{F}_J^p = ES_J\frac{\|\vec{X}_{J_p}-\vec{X}_J\|-l_{op}}{l_{op}}\frac{\vec{X}_{J_p}-\vec{X}_J}{\|\vec{X}_{J_p}-\vec{X}_J\|} \tag{54}$$

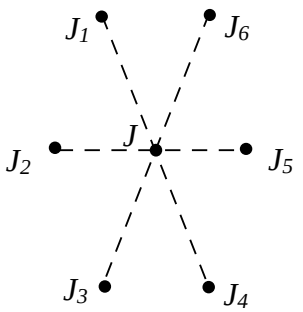

Fig. 11. Description of the net sheet: the set of neighbouring nodes.

where S_J is the cross-section of the individual wires joining nodes J and J_p, l_{op} is their initial length, and E is the elastic modulus of the steel. It is assumed that F_J^p is a tension force; thus, if $\| \overrightarrow{JJ}_p \| < l_{op}$, F_J^p is equal to zero.

3.3.3. Mechanical interaction between snowpack and net structure

Modelling the interaction between a snow mantel and a structure appears to be a boundary problem in which the structure is a complex boundary for the snowpack. The interaction between the snowpack and the net sheet is obviously not reduced at a single point, as suggested previously. In fact, the wires that constitute the net sheet have a cross-section which must not be ignored. Furthermore, because of complex local phenomena occurring at the interface between the net and the snow, the actual open sections through the wire mesh may be reduced. This suggests that each node J is associated with a closed section (denoted J), so that any snow element that is in contact with this section does not go through it (Fig. 12). This expansion of sections around nodes accounts for the longitudinal surface of the different wires. Indeed, in the proposed approach, wires are described only with nodes located at the connection points. However, interaction between the net and the snowpack can also occur on the longitudinal part of the wires between two adjoining connection nodes. From a physical point of view, as the cross size of the wires is quite small, snow in the vicinity of the wires tends to glide around them, inducing volumetric strains in the snow, as well as a dissipation of energy. In the proposed model, kinematic assumptions concerning the snowpack do not account for this glide. Thus, assuming that some snow elements are blocked upstream of wires turns out to be an expedient manner to take a dissipation of energy into account: this dissipation of energy takes place at the interface between the moving snow elements and those blocked upstream of the wires.

Furthermore, it is assumed that during contact between a snow element I and a closed section J, this section does not penetrate the snow element. Thus, at each time, the incremental displacements in direction $\vec{k}_1$ of the two bodies I and J are equal:

$$\mathrm{d}\vec{X}_J \cdot \vec{k}_1 = \mathrm{d}u_I \tag{55}$$

This kinematic condition makes it possible to model the slowdown of the mantel, and Eq. (55) allows reaction force R_I to be computed.

3.3.4. Boundary conditions

The snowpack has a parallelepiped shape, and thus appropriate boundary conditions have to be adjoined on the six-plane surface. The frontal plane is in interaction with the structure and was described in the previous section. At the interface between the mantel and the soil, the Coulomb friction law is introduced, so that the sliding between the two bodies can be modelled; this law requires the friction angle φ_s to be known. The back plane and the upper surface of the mantel are assumed to be free, which means that no stresses are applied to them. The two lateral planes can be chosen free or blocked.

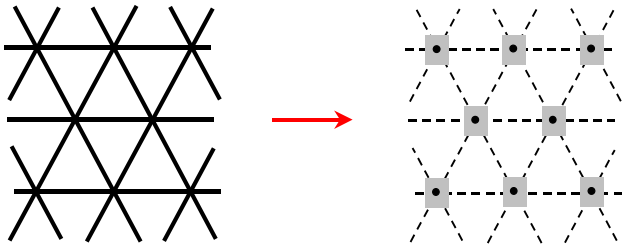

Fig. 12. Introduction of a closed section located at each node.

4. Concluding remarks

This paper has proposed a multiscale approach for inferring the global behaviour of a snow cover from its local properties. Although a very simple model is used to describe the local behaviour of the grain bonds, a complex overall behaviour is obtained by taking a statistical description of the fabrics into account. One major advantage lies in the fact that only a few parameters are included in this model. However, it must be noted that this model is based on the following assumptions:

- The mechanical behaviour of a snow volume element depends only on the mechanical behaviour of the inter-granular bonds belonging to this volume.
- The local behaviour of the inter-granular bonds, described as a quasi-brittle material, is designated by a non-linear tensile–compressive visco-elastic model.
- Shear strength of grain bonds is ignored.
- The strain localization operator was inferred using an affine approximation from the macroscopic strain tensor.
- The local fabric of the medium is described well by both the mean coordination number and the distribution densities f_θ and f_φ of inter-granular bond orientations.

Furthermore, the constitutive equations have been entirely determined in the case of a snow mantel in interaction with a flexible structure. As a first step, a local simple linear visco-elastic law was used, allowing the explicit analytical constitutive formulation to be inferred. But the extension to the non-linear case is also proposed. More complex local models should be examined in the future. As a direct experimental study of the snowpack remains a very difficult task, it should be meaningful to use a structure in order to indirectly obtain information related to the snowpack. In these conditions, the net structure acts as a macroscopic but relevant sensor. Mechanical modelling of the interaction between the snowpack and the net structure has led to a Lagrangian approach based on the discrete-element method. This type of description seems to be meaningful and of a great interest for cable structures such as avalanche net structures. The relevance of discrete modelling of the snowpack is closely related to the validity of the proposed form of the displacement field of the snowpack. As confirmed in Part II, which follows, the complete modelling method is capable of a very good simulation of the forces acting in the different parts of the structure.

References

Bader, H. et al., 1939. Der schnee und seine metamorphose. USA Snow Ice and Permafrost Research, available from the National Technical Information Service.

Bardet, J.P., 1998. Introduction to computational granular mechanics. In: Cambou, B. (Ed.), Behaviour of Granular Materials. Springer Wien, New York, pp. 99–169.

Bartelt, P., Christen, M., submitted for publication. A computational procedure for instationary temperature-dependent snow creep.

Bazant, Z., Prat, P., 1988. Microplane model for brittle-plastic material. ASCE Journal of Engineering Mechanics 114 (10), 1673–1702.

Billaux, D., Cundall, P.A., 1993. Modeling of geomaterials using the Lagrangian Element Method. Revue Française de Géotechnique 63, 9–21.

Brown, R.L., Edens, M.Q., 1991. Changes in the microstructure of snow under large deformations. Journal of Glaciology 37 (126), 193–202.

Brun, E., Martin, E., Simon, V., Gendre, C., Coléou, C., 1989. An energy and mass model of snow cover suitable for operational avalanche forecasting. Journal of Glaciology 35 (121), 333–342.

Caillerie, D., 1995. Evolution quasistatique d'un milieu granulaire, loi incrémentale par homogénéisation. In: Des matériaux aux ouvrages. Hermès, Paris, pp. 53–80.

Cambou, B., 1998. Micromechanical approach in granular materials. In: Cambou, B. (Ed.), Behaviour of Granular Materials. Springer Wien, New York, pp. 170–216.

Cambou, B., Dubujet, P., Emeriault, F., Sidoroff, F., 1995. Homogenization for granular materials. European Journal of Solids, A/Solids 14 (2), 255–276.

Castelnau, O., 1996. Modélisation du comportement mécanique de la glace poly-cristalline par une approche auto-cohérente, application au développement de textures dans les glaces des calottes polaires. Thesis, Univ. Joseph Fourier, Grenoble, France.

Chang, C.S., Liao, C.L., 1994. Estimates of elastic modulus for media of randomly packed granulates. Applied Mechanics Review 47, 197–206.

Cundall, P.A., Roger, D.H., 1992. Numerical modelling of discontinua. Engineering Computations 9, 101–113.

Desrues, F., Darve, F., Flavigny, E., Navarre, J.P., Taillefer, A., 1980. An incremental formulation of constitutive equations for deposited snow. Journal of Glaciology 25 (92), 289–307.

Duva, J.M., Crow, P.D., 1994. Analysis of consolidation of reinforced materials by power-law creep. Mechanics of Materials 17 (1), 25–32.

Gagliardini, O., Meyssonnier, J., 1997. Flow simulation of a firn-covered cold glacier. Annals of Glaciology 24, 242–248.

Gagliardini, O., Meyssonnier, J., 1999. Analytical derivations for the behavior and fabric evolution of a linear orthotropic ice polycrystal. Journal of Geophysical Research 104, 17,797–17,809.

Hansen, A.C., Brown, R.L., 1987. A new constitutive theory for snow based on a micromechanical approach. In: Avalanche Movement and Effects, Proceedings of the Davos Symposium, IAHS Publication no. 162, pp. 87–104.

Hill, R., 1967. The essential structure of constitutive laws for metal composites and polycrystals. Journal of the Mechanics and Physics of Solids 15, 79–95.

Kern, F., 1978. Calcul des efforts dans les filets paravalanches. Compte rendu de la seconde deuxième rencontre internationale sur la neige et les avalanches, ANENA, Grenoble, pp. 241–250.

Kragelski, I.V., Shakhov, A.A., 1949. Change of the mechanical properties of a snow surface as a function of time. In: The Physico-Mechanical Properties of Snow and Their Application in the Construction of Airfields and Roads. Academy of Sciences, Moscow, pp. 6–9. Translation by Bureau of Yards and Docks, Washington.

Kry, P.R., 1975. The relationship between the visco-elastic and structural properties of fine-grained snow. Journal of Glaciology 14 (72), 467–477.

Larsen, J.O., 2000. Design Criteria for Cylindrical Masts Exposed to Snow Creep Forces, Snow Engineering. Balkema, Rotterdam. pp. 105–112.

Lemaitre, J., Chaboche, J.L., 1988. Mécanique des matériaux solides. Ed. Dunod, Paris. pp. 163–249.

Lewis, H.S. et al., 1997. Snow mechanics, review of the state of knowledge and applications. CRREL Report 97.3, pp. 1–34.

Lliboutry, L., Duval, P., 1985. Various isotropic and anisotropic ices found in glaciers and polar ice caps and their corresponding rheologies. Annals of Glaciology 3 (2), 207–224.

Margreth, S., 1995. Snow Pressure Measurements on Snow Net Systems. Actes de colloque, Chamonix. pp. 241–248.

Masson, S., Martinez, J., 2000. Multiscale simulations of the mechanical behaviour of an ensiled granular material. Mechanics of Cohesive-Frictional Materials 5 (6), 425–442.

Mellor, M., 1975. A review of basic snow mechanics. IAHS-AISH Publication no. 114, Snow Mechanics Symposium, Grindelwald, pp. 251–291.

Nicot, F., 1999. Etude du comportement mécanique des ouvrages souples de protection contre les éboulements rocheux. Thèse de troisième cycle, Ecole Centrale de Lyon.

Nicot, F., submitted for publication. Constitutive modelling of snow from a micro-mechanical description. Journal of Glaciology.

Nicot, F., Gay, M., Tacnet, J.M., 2002. Interaction between a snow mantel and a flexible structure, a new method to design avalanche nets. Cold Regions Science and Technology 34, 67–84.

Pimienta, P., 1987. Etude du comportement mécanique des glaces poly-cristallines aux faibles contraintes, application aux glaces des calottes polaires. Thesis, Univ. Sci. Tech. et Med. de Grenoble, France.

Salm, B., 1975. A constitutive equation for creeping snow. IAHS-AISH Publication no. 114, Snow Mechanics Symposium, Grindelwald, pp. 222–235.

Sidoroff, F., 1984. Comportement des matériaux. Ecole Centrale de Lyon.

St. Lawrence, W.F., 1980. The acoustic emission response of snow. Journal of Glaciology 26 (94), 209–216.